# Temporal Fluctuations in Single-Molecule SERS Spectra

Anna Rita Bizzarri and Salvatore Cannistraro

Biophysics and Nanoscience Centre, CNISM, Dipartimento di Scienze Ambientali, Universita' della Tuscia, I-01100, Viterbo, Italy
{bizzarri,cannistr}@unitus.it

## 1 Introduction

New advances in ultrasensitive spectroscopy, able to detect a single molecule (SM), are of utmost interest in different disciplines from both fundamental and application aspects [1, 2, 3]. Earlier SM fluorescence studies at ambient conditions, showed blinking, spectral jumps, intensity fluctuations, yielding thus new insight into phenomena usually wiped out in ensemble average [4, 5].

Although Raman spectroscopy is characterized by an extremely low cross section, SM detection can be reached when the molecules are adsorbed onto metallic surfaces with nanometer-scale roughness or onto metal nanoparticles [6, 7]. Such an approach, called surface-enhanced Raman spectroscopy (SERS), gives rise in a drastic increase of the Raman cross section (up to $10^{14}$) [8, 9, 10], as due to two, likely cooperating, mechanisms: an electromagnetic (em) local field enhancement and a charge transfer (CT) between the molecule and the metal surface [6, 7]. The latter, which requires a tight, chemical interaction between the molecule and the metal [11, 12], has been recently suggested to play a dominant role in SM SERS spectra [13]. With respect to other SM spectroscopies, SERS is endowed with a high sensitivity coupled to a rewarding chemical and structural specificity [14]. Therefore, SERS is one of the most sensitive spectroscopic approaches available for analytical chemistry, nanomedicine and nanotechnology [15, 16].

SERS spectra in the SM regime exhibit drastic temporal fluctuations in both line intensity and frequency [17, 18]. The vibrational mode emission of a SM has been shown to undergo a characteristic intermittent behavior that might encode both the dynamics of the molecule and the details of its interaction with the environment [19]. Information about the structural conformations sampled by the molecule can also be obtained; this being particularly relevant for proteins, due to the complex energy landscape explored during their dynamical evolution [20].

Therefore, an investigation of the SM spectral fluctuations, based also on suitable statistical approaches, may help in addressing some fundamental issues, such as ergodicity, statistical aging, entanglement of vibrational modes, nonstationarity of the emission processes, etc. [21, 22, 23]; these being of high relevance for a detailed knowledge of the fundamental dynamical processes in

K. Kneipp, M. Moskovits, H. Kneipp (Eds.): Surface-Enhanced Raman Scattering – Physics and Applications, TAP 103, 281–298 (2006)

molecular systems [24]. Moreover, an analysis of SM SERS fluctuations could also lead to new insights into the charge or electron-transfer (ET) mechanisms regulating the molecule–metal interaction under light excitation [25]. Such an aspect may deserve some interest to unravel the role played by the CT in SERS and even in the interfacial photophysical processes occurring in optoelectronic devices [26, 27].

On such a basis, we have performed a statistical analysis on the intensity and frequency fluctuations of SERS spectra of single Myoglobin (Mb) and protoporphyrin IX (FePP) molecules adsorbed onto silver nanoparticles. Such an analysis has allowed us to investigate the role of the continuum background, underneath the SERS spectra, on the intensity fluctuations.

The spectral jumps observed in the FePP vibrational modes that are fingerprints of the iron oxidation states, evidenced a light-induced, reversible, ET occurring between the molecule and the metal surface. These SERS experiments have also been conjugated with scanning tunneling microscopy (STM) measurements to closer elucidate the ET properties of the molecules at a metal surface.

An analysis of the temporal emission of most of the molecular vibrational modes has shown a random switching from a bright (on) state to a dark (off) state under continuous laser excitation. The probability distribution associated with the time intervals between the off states follows a power law that has been traced back to a Lévy statistics. Such a behavior has been suggested to arise from an anomalous diffusion of the FePP molecule on the metal surfaces, likely in connection with a modulation of the CT between the molecule and the metal. Furthermore, the presence of the protein milieu around the heme group has been shown to induce a higher variability on the intensity fluctuations of the heme vibrational modes.

All these findings constitute a new insight into both the photophysical behavior of molecules and their interaction with the nanoenvironment.

## 2 Materials and Methods

Solutions of colloidal silver were prepared by standard citrate reduction of $AgNO_3$ (Sigma) by following the procedure of *Lee* and *Meisel* [28]. The concentration of the silver colloidal particles, estimated from the optical extinction spectrum, was about $10^{-11}$ M, corresponding to about $7 \times 10^{12}$ particles per liter. As activation agent NaCl was added to reach the final concentration of 0.25 mM. FePP (Sigma) was dissolved into a KOH solution 0.5 M at pH = 12 and $10^{-6}$ M. Purified horse Mb (Sigma) was dissolved into a phosphate buffer solution at pH 6.8 and a concentration of 1 mM. An aliquot of successive dilutions of each of these solutions was incubated with silver colloidal suspension for 3 h at room temperature to obtain a final concentration of $10^{-11}$ M with an approximate ratio of 1 : 1 between molecules and colloidal particles. The samples were obtained from a 10 µl droplet of these solutions

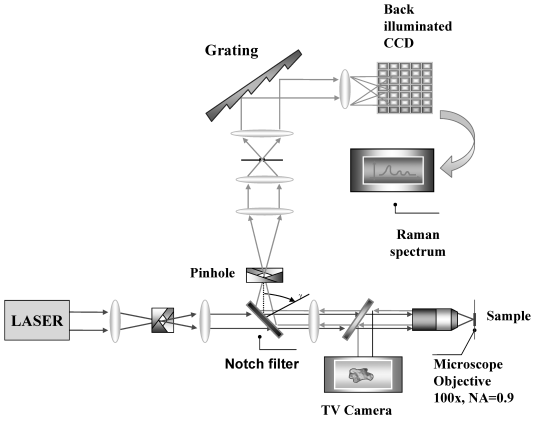


**Fig. 1.** A schematic representation of the Raman equipment

deposited onto a glass slide, of area $15 \times 15\,\mathrm{mm}^2$, coated with polymerized 3-aminopropyltriethoxysilane (APES, Sigma) and, finally, dried. A characterization of immobilized silver colloidal particles, performed by atomic force microscopy (AFM) under ambient conditions, revealed single spherical and rod-shaped particles and aggregates of two, three, up to many particles; the heterogeneous particle-size distribution being characterized by an average of about 70 nm [29]. Silver STM tips, prepared by cutting a silver wire, were washed in acetone, ethanol, and finally in ultrapure water, and incubated for 1 h at room temperature with an FePP solution at $10^{-9}$ M.

SERS spectra were collected with a confocal SuperLabram (Jobin–Yvon) equipment using the 514.5 nm radiation line of an argon laser. The illumination and backscattering collection system consisted of a confocal microscope coupled to a single-grating spectrometer (300 mm focal length spectrograph with a 1800 grooves/mm grating) and a liquid-nitrogen-cooled backilluminated CCD detector; a schematic representation of the equipment is shown in Fig. 1.

The microscope objective was 100× with NA = 0.9, producing a laser spot size of about 1 μm in diameter. The spectral resolution is better than $5\,\mathrm{cm}^{-1}$. The laser power was varied from 0.1 mW to 8 mW, resulting into a range of 0.01 mW to 0.8 mW for the power impinging on the sample. The spectra were collected in sequence with 1 s of integration time and 1 s from one measurement to the next by an automatic acquisition routine.

Tunneling spectroscopy was performed with a PicoSPM (Molecular Imaging). I–V curves were recorded on FePP adsorbed on silver tips in close proximity to a freshly cleaved highly oriented pyrolitic graphite (HOPG) electrode in a nitrogen atmosphere. The scan was disabled and the tip set at a tunneling resistance of $4 \times 10^{10}\,\Omega$ (200 mV, 5 pA).

The total noise $N_{\mathrm{t}}$ of a SERS signal can be determined as the root of the sum of the square noise components:

$$N_{\mathrm{t}} = [N_{SN}^2 + N_R^2 + N_D^2]^{\frac{1}{2}}, \tag{1}$$

where the readout noise $N_{\mathrm{R}}$, and the dark charge noise $N_{\mathrm{D}}$, are specified by the chip manufacturer; $N_{\mathrm{SN}}$ is the shot noise associated with the signal and whose amplitude is given by the square root of the measured signal. For our CCD chip, $N_{\mathrm{R}}$ was 5 electrons rms and $N_{\mathrm{D}}$ one electron/pixel/h. The CCD chip had, at a wavelength of 514.5 nm, a quantum efficiency of about 0.92 with one count per two collected photons. In a typical SM SERS experiment, a rate of about 100–400 counts per second are usually detected; the raw data including an underlying continuum. Accordingly, a total noise, dominated by the shot noise, of about 7–18 counts is expected for measurements obtained for an integration time of 1 s [8, 30]. As long as the shot noise is dominant, a Poisson distribution with a standard deviation equal to $N_{\mathrm{t}}$, is expected to describe the spread of the Raman intensity around the average value.

## 3 Results and Discussion

### 3.1 Fluctuations in SM SERS Spectra

Scanning the sample area under the microscope objective of the Raman equipment, generally reveals emitting sites with a different average intensity. Most of these sites are characterized by an intensity almost equivalent to that of the noise. Only a few bright emitting sites, usually called hot spots, corresponding to about 1 % of the total, are observed.

Figure 2 shows a sequence of SERS spectra with 1 s of integration time and excited at a wavelength of 514.5 nm, from a typical bright site of immobilized Ag colloids incubated with FePP at $10^{-11}$ M. From spectrum to spectrum, there is a great variability in both the relative peak intensity as well as in the peak frequency. Lines appear and disappear suddenly and the peak intensity, as well as the frequency of the lines, drastically change in time; similar results having been obtained for Mb [29] and cytochrome c [31], at the SM level. The emission behavior resembles that found in the SM SERS spectra of heme-proteins [31, 32, 33], of green fluorescent protein [34], and of other organic molecules [17, 18, 35].

The drastic fluctuations and blinking of modes, in connection with the extremely low concentration of molecules present in the initial solution (an average number of less than one molecule in the laser-illuminated spot is estimated [18, 31]) are indicative that SM detection has been reached in our SM SERS spectra, in agreement with what was found in the literature [18,32].

Figure 3a and 3b show the spectra obtained by summing up a large number of successive SM SERS traces from single Mb and FePP molecules,

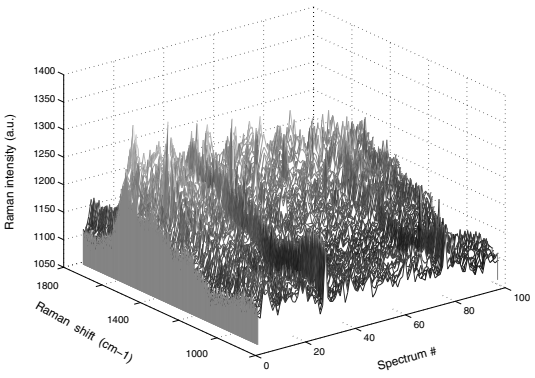


**Fig. 2.** A sequence of 100 SERS spectra with l s of integration time from a bright site of immobilized silver colloidal particles incubated with FePP at a concentration of $10^{-11}$ M

respectively. These spectra appear very similar to those taken from a dried droplet of bulk solutions ($10^{-4}$ M) (see dashed lines in Fig. 3). The almost complete recovery of the bulk vibrational spectra, reached either by summing several SM spectra or, equivalently by using a long integration time, suggests a substantial ergodicity of the system, and that no significant photodegradation has occurred in our sample during the measurements. However, in a few cases, the SERS signals become dominated by two characteristic, high-intensity, peaks at about 1350 $\mathrm{cm}^{-1}$ and 1580 $\mathrm{cm}^{-1}$. These peaks, usually attributed to carbon contamination [36], might arise from a photoinduced degradation of aromatic molecules [37]; these SERS series having been discarded in the further analysis.

### 3.2 Statistical Analysis of Intensity Fluctuations in SM SERS Spectra

As already mentioned, intensity and spectral fluctuations in SM SERS spectra may encode information about both the dynamics of the molecule and its interactions with the environment including the metal surface. We have taken into account the intensity fluctuations of the vibrational modes of FePP and Mb.

Figure 4 shows the intensity as a function of time (a), and the related histograms (b), of two of the most intense vibrational modes of Mb and FePP [38]: the iron spin marker $\nu_3$ (at around 1480 $\mathrm{cm}^{-1}$) and the vinyl stretching mode $\nu_{10}$ (at around 1620 $\mathrm{cm}^{-1}$). For comparison, the same analysis has been performed at 1800 $\mathrm{cm}^{-1}$, where no Raman signal is registered. Drastic temporal fluctuations for both of the molecules are observed at all three frequencies. Such a recurrent feature of the SERS spectra at the SM level [17, 18] discloses processes strongly modulating the Raman scattering of

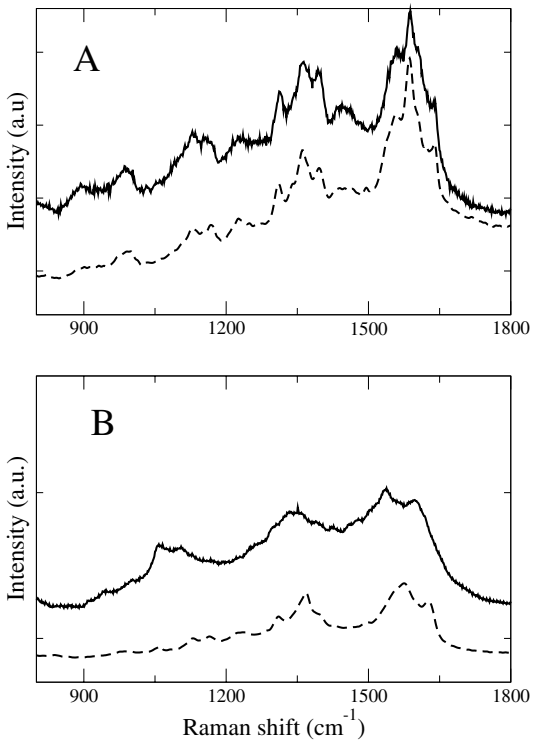


**Fig. 3.** (**a**) *Continuous line*: Collection of 600 1 s SERS spectra from immobilized silver colloids incubated with Mb at $10^{-11}$ M. *Dashed line*: Raman spectrum from a dry droplet of bulk Mb ($10^{-4}$ M in phosphate buffer) with 60 s of integration time. (**b**) *Continuous line*: Collection of 600 1 s SERS spectra from immobilized silver colloids incubated with FePP at $10^{-11}$ M. *Dashed line*: Raman spectrum from a dry droplet of bulk FePP ($10^{-4}$ M in alkaline aqueous medium) with 60 s of integration time. The SERS spectra were recorded in sequence lasting 1 s between two successive measurements. The spectral resolution is better than 5 $cm^{-1}$

the molecules at the metal surface. The histograms of Fig. 4b are consistent with a single-mode distribution for all the analyzed lines of the two systems. From the analysis of the distribution spread, quantified by their standard deviations, some observations can be made: 1. The standard deviations measured at 1480 $cm^{-1}$ and 1620 $cm^{-1}$ are found to be higher than those at 1800 $cm^{-1}$ that, in turn, significantly exceed the values expected from the CCD noise (see values in Fig. 4b). The intensity fluctuations at 1800 $cm^{-1}$, where no Raman lines occur, monitor the variability of the continuum background that always underlies the SERS lines [10, 18] (see also below). On the other hand, the intensity fluctuations detected at 1480 $cm^{-1}$ and 1620 $cm^{-1}$ are expected to arise from the variability of both the continuum background and the specific vibrational modes; the latter encompassing the intrinsic dy-

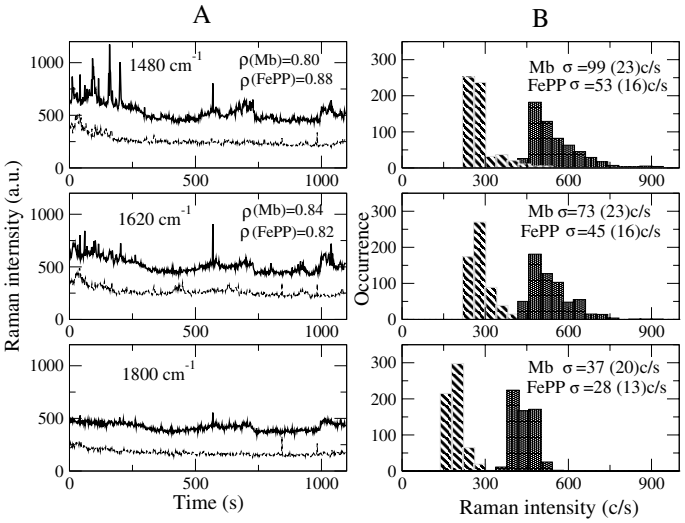


**Fig. 4.** (**a**) Intensity, as a function of time, detected at $1480\,\mathrm{cm}^{-1}$, $1620\,\mathrm{cm}^{-1}$, and $1800\,\mathrm{cm}^{-1}$ from SM SERS spectra of Mb (*black lines*) and FePP (*gray lines*). The values of the crosscorrelation $\rho$ between the intensity at $1480\,\mathrm{cm}^{-1}$ and $1800\,\mathrm{cm}^{-1}$ and at $1620\,\mathrm{cm}^{-1}$ and $1800\,\mathrm{cm}^{-1}$ were calculated by (2). (**b**) Histograms of data in (**a**) for Mb (*dark pattern*) and for FePP (*dashed pattern*). $\sigma$ indicates the standard deviations of the data; in parentheses the corresponding $\sigma$ values expected from the CCD noise (see (1))

namics of the molecule, and its interaction with the environment. 2. The standard deviations related to Mb appear higher than those of FePP. Actually, the presence of the protein, which dynamically explores the complex energy landscape of its conformational substates [20], reasonably leads to a larger variability of the heme group vibration intensities [29, 31].

On visual inspection, the intensity trend of the three frequencies in Fig. 4a seems to indicate that the Raman emissions are strongly correlated in time; drastic intensity jumps simultaneously occurring at the three frequencies for Mb and FePP. The same trend in time has also been observed for the other main vibrational modes and even for the total intensity [18]. To quantify such a correlation, we have evaluated the crosscorrelation, between the intensities at the two frequencies $\nu_1$ and $\nu_2$, at a 0 time delay [39]:

$$\rho_{\nu_1,\nu_2} = \frac{\sigma_{\nu_1,\nu_2}}{\sigma_{\nu_1}\sigma_{\nu_2}}, \tag{2}$$

where $\sigma_{\nu_1}$ and $\sigma_{\nu_2}$ are the standard deviations of the intensity at $\nu_1$ and $\nu_2$, respectively, and $\sigma_{\nu_1,\nu_2}$ is the covariance given by:

$$\sigma_{\nu_1,\nu_2} = \frac{1}{N}\sum_i [I_i(\nu_1) - \overline{I(\nu_1)}][I_i(\nu_2) - \overline{I(\nu_2)}]\,. \tag{3}$$

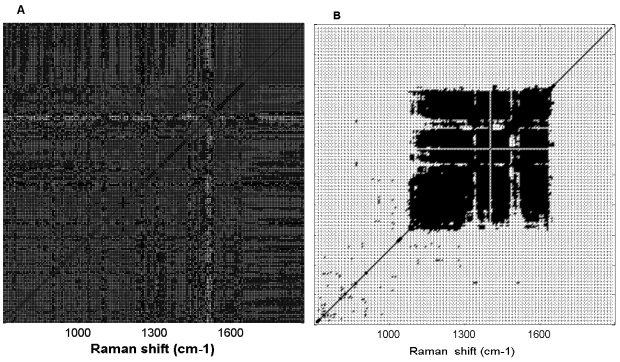


**Fig. 5.** Two-dimensional crosscorrelation map (see (2)) from a series of 600 SERS spectra of FePP obtained from (**a**) the raw data and (**b**) after removing the continuum background. The continuum background has been removed from each spectrum by subtracting the intensity measured at $1800\,\mathrm{cm}^{-1}$ at all frequencies. *Dark points* mark regions, over a grating, with crosscorrelation values higher than 0.8

$I_i(\nu_j)$ $(j = 1, 2)$ is the Raman intensity, detected at the wavelength $\nu_j$ at time $t_i$; $\overline{I(\nu_j)}$ is the Raman intensity, at the wavelength $\nu_j$, averaged over all the measurement time intervals. Accordingly, high $\rho_{\nu_1,\nu_2}$ values indicate that the intensity at $\nu_1$ fluctuates, around the average, in parallel with the intensity at $\nu_2$.

The crosscorrelation, calculated by (2), between the two intensities at $1480\,\mathrm{cm}^{-1}$ and $1620\,\mathrm{cm}^{-1}$ is found to be higher than 0.8 for both Mb and FePP (see the legend of Fig. 4). Strikingly enough, similar high correlation values are also obtained for the crosscorrelation between the $1800\,\mathrm{cm}^{-1}$, and the $1480\,\mathrm{cm}^{-1}$ or $1620\,\mathrm{cm}^{-1}$ intensities (see values in Fig. 4). Furthermore, high correlation values are observed for the intensities between each couple of frequencies of the FePP SERS spectrum. This can be visualized from the two-dimensional (2D) map, shown in Fig. 5a, where crosscorrelation values higher than 0.8 are detected throughout almost all the frequency range.

Such a high correlation finds a correspondence with that reported for rhodamine [40], for which it has been put into relationship to the presence of SERS signals due to bare colloids. These results, also in connection with a variability at $1800\,\mathrm{cm}^{-1}$ higher than that due to the noise, suggest that the continuum significantly contributes to the intensity modulation of the vibrational-mode intensities. Provided that such a background is not due to fluorescence, commonly affecting Raman spectra and quenched when molecules are adsorbed onto metal surfaces [7, 41], several hypotheses have been put forward about its origin. Indeed, it could be suggested to arise from an electronic scattering from the metal [42], or from a byproduct of a nonradiative CT process between the surface and the molecule [12].

To put into evidence the correlation between the real FePP signals, we have to get rid of the continuum background. Figure 5b shows the map of the 2D crosscorrelation after having removed the continuum background from each spectrum. Correlation values higher than 0.8 are detected only at the crossing points between the frequencies of the main FePP vibrational modes, at variance with what is observed in Fig. 5a, in which a specific intensity correlation was observed. The evidence that a high correlation in the intensity of the FePP vibrational modes persists after removing the continuum, suggests a common origin for their intensity fluctuations. It could be hypothesized that the intensity fluctuations of the specific vibrational modes could be driven by the correspondent fluctuations of the enhancement factor. In particular, the presence of the continuum could be connected to the SERS mechanism, through, for example, a CT process between the molecule and the metal surface, in good agreement with the recent findings supporting the dominant role of the CT to obtain SM SERS signals [13].

### 3.3 ET in SM SERS Spectra of FePP

The capability of FePP iron to switch from $Fe^{2+}$ to $Fe^{3+}$ and backwards, when illuminated in the presence of a metallic surface, can have a high impact from an application standpoint. Indeed, FePP has been proposed to be a suitable, robust molecular element for assembling electronic and photonic nanodevices [43, 44]. Furthermore, the iron oxidation state of FePP, which constitutes the prosthetic group of several metalloproteins, plays a key role in many biological functions [45]. Therefore, it would be interesting to follow the temporal evolution, at the SM level, of the vibrational markers of the iron oxidation state in FePP. We have then focused our attention on the spectral region of the $\nu_4$ band, corresponding to the pyrrole half-ring vibration, marker of the heme iron oxidation state. In bulk, this band is peaked at $1363\,\mathrm{cm}^{-1}$ for the iron ferrous state, and at a higher frequency, $1375\,\mathrm{cm}^{-1}$, for the ferric state [38]. The intensity detected at both these frequencies, reveals drastic jumps, as a function of time, similarly to what was previously shown for the other vibrational modes. Moreover, a temporal analysis of the peak occurrence at each of the two frequencies (see Fig. 6 and its legend), indicates that the two peaks are alternatively observed in almost all the spectra registered in a time sequence. A few cases with a simultaneous detection of both lines have also occurred (triangles in Fig. 6).

The observed bimodal behaviour in the peak appearance can be linked to a fast and reversible change in the oxidation state of the FePP iron ion during the measurement [46, 47]. The detection of both the oxidation states in a single spectrum, observed for a few cases, can be due to a switching between $Fe^{2+}$ and $Fe^{3+}$ during the integration time.

Further information about the ET properties of FePP at a metal interface, can be obtained by performing a SERS/STM combined experiment in which FePP is adsorbed on a silver STM tip. Therefore, it has been verified that

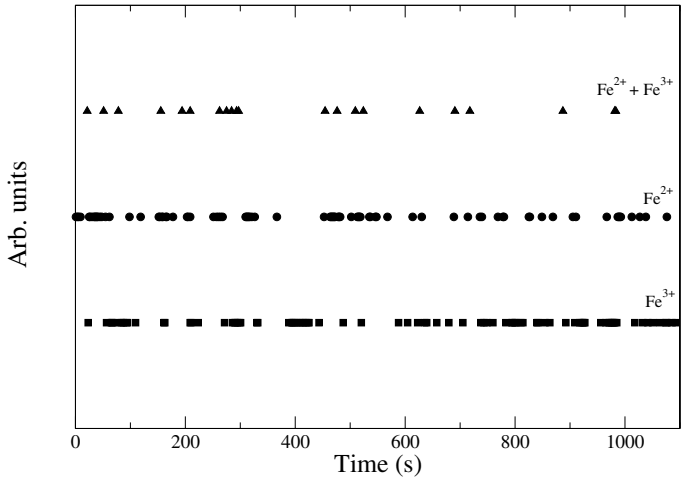


**Fig. 6.** Appearance of Raman peaks, over the continuum background, as a function of time, in SM SERS spectra of FePP, at 1363 $cm^{-1}$ (*squares*), at 1375 $cm^{-1}$ (*circles*) and at both 1363 $cm^{-1}$ and 1375 $cm^{-1}$ (*triangles*). A peak at a given frequency is detected when its intensity overcomes the threshold of $2\sigma$ above the noise level of the spectrum

the tip roughness is suitable to yield a huge SERS enhancement down to SM detection; the occurrence of ET, similarly to what was observed with silver colloids, having also been revealed [25]. Then, we have investigated the electron flow in the molecule–tip tunneling junction, mounted on a STM equipment.

The recorded $I$–$V$ curve is shown in Fig. 7a (continuous line) together with data related to a bare tip (dashed line). The tunneling current as a function of the bias in the presence of FePP appears markedly asymmetric, increasing rapidly up to about 0.8 nA for negative bias lower than −0.7 V, while it remains small in reverse bias. By contrast, the tunneling curve for the bare silver tip is highly symmetric, with the absolute current intensity smaller than 0.2 nA. Generally, the observed trend for the $I$–$V$ curve, indicative of a diode-like curve (current rectification) [48], reflects the redox properties of the molecule [49, 50]. Then, the current flowing through the tunneling junction obtained by approaching the tip to a HOPG substrate has been recorded in a sequence of 10 s at a fixed bias of −0.2 V, with the feedback control transiently disabled. While the current recorded on a bare tip is almost constant with very small fluctuations, on the contrary, the FePP–tip system exhibits drastic tunneling-current fluctuations (see Fig. 7b). The reported results on an FePP molecule adsorbed onto a silver tip are indicative of a significant variability in the tip–molecule substrate junction during the tunneling experiments, and are closely reminiscent of the variability observed in SM SERS spectra.

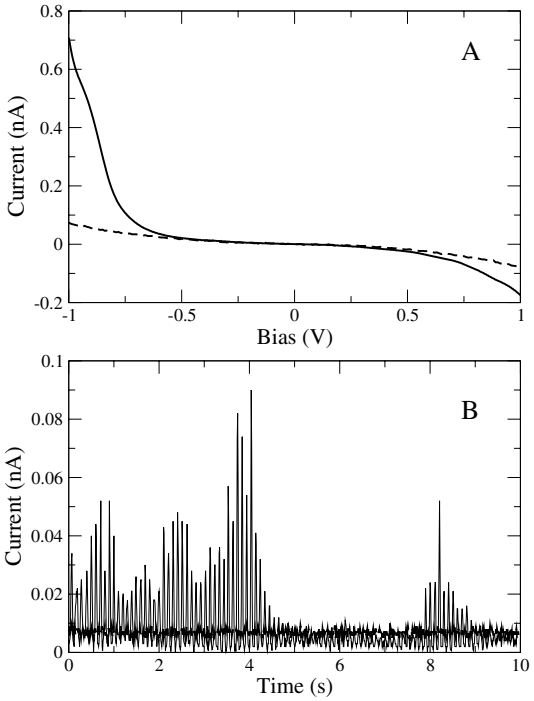


**Fig. 7.** (**a**) *I–V* characteristics as recorded by tunneling spectroscopy of FePP–tip (*solid line*) and bare tip (*dashed line*). Measurements were performed under nitrogen atmosphere at a starting tunneling resistance of $4 \times 10^{10}\,\Omega$ (bias, 0.2 V; tunneling current, 5 pA). (**b**) Tunneling current, as a function of time, at −0.2 V bias for bare tip (*black curve*) and for a silver tip incubated with FePP (*gray curve*)

The switching of the iron oxidation state of FePP could be induced by visible light that triggers a nonradiative CT between the FePP molecule and the silver surface. Such a picture finds a correspondence with the Otto–Persson model for which ballistic electrons generated via excitation of the surface plasmon couple to the chemisorbed molecule [12, 42]. In other words, ballistic electrons from the silver surface could jump nonradiatively towards the FePP molecule and backwards. In this framework, the highest occupied molecular orbital (HOMO) and the lowest unoccupied molecular orbital (LUMO) of the adsorbed molecule should be symmetrically located in energy with respect to the Fermi level of the metal that acts as an initial or final state in the resonance Raman process [7, 12, 42]. Therefore, only molecules with low-lying LUMO levels can interact with ballistic electrons giving rise to high SERS signals [51]. The related positions among the HOMO, LUMO levels and the Fermi energy of the FePP could be slightly modulated by different factors, such as the presence of oxygen or some doping elements, and the arrangement of the molecule with respect to the surface [7, 46]. Furthermore, the

observed fluctuations in the tunneling current, reflecting a variability in the electronic coupling between the molecule and the metal, can be traced back to migrations of the molecule and/or changes of the molecule orientations with respect to the metal surface during the measurements.

Finally, we mention that the occurrence of an ET between FePP and the metal surface could provide a support to the CT mechanism in yielding the SERS enhancement required in the SM regime [13].

### 3.4 Lévy Statistics in SM SERS Spectra of FePP

At first glance, the intermittent behavior of the vibrational modes in SM SERS signals appears to be essentially erratic. However, it would be interesting to assess if some law could be hidden in this phenomenon. To such a purpose, we have focused our attention on the appearance and disappearance of three main vibrational modes in the SERS spectrum of single FePP molecules.

The vertical lines in Fig. 8 mark the times, within the acquisition sequence, at which peaks at $1480\,\mathrm{cm}^{-1}$, $1570\,\mathrm{cm}^{-1}$ and $1620\,\mathrm{cm}^{-1}$ are detected. These peaks reveal a binary trace (intermittence), which is common to the other vibrational modes. This means that the molecular vibrational modes may switch from a bright (on) state to a dark (off) state under continuous laser excitation. Notably, no correlation (or anticorrelation) among the temporal emission of the three peaks is registered (see also legend of Fig. 8). Accordingly, it can be suggested that the various vibrational modes follow independent activation channels during the temporal evolution of the molecule dynamics.

To analyze the statistical properties of the on/off state occurrence for the selected vibrational emission modes, we have collected for ten spectra series in sequence, the time intervals, $\tau_{\mathrm{off}}$, during which no peak is revealed in the series of spectra for each analyzed frequency. The $P_{\mathrm{off}}$ distributions, calculated by evaluating the occurrence of the corresponding $\tau_{\mathrm{off}}$ within the acquisition time, are well described by a power law (continuous lines in Fig. 9a):

$$P_{\mathrm{off}} \sim 1/\tau_{\mathrm{off}}^{(1+\alpha)}, \tag{4}$$

with $\alpha$ values ranging from 0.46 to 0.56. The assessed independence of the $\alpha$ exponents on the laser intensity rules out the possibility that such an effect could be due to irreversible photoinduced processes [37]. The observed non-exponential behavior of the $P_{\mathrm{off}}$ distribution suggests some space–temporal heterogeneity in the off (dark) state of the FePP vibrational modes [52]. Indeed, the presence of a single off state would have given rise to a simple exponential decay for $P_{\mathrm{off}}$ [53]. On the other hand, the rather similar temporal decay observed for the three lines suggests that, although the vibrational modes may follow a different activation channel, a common mechanism is

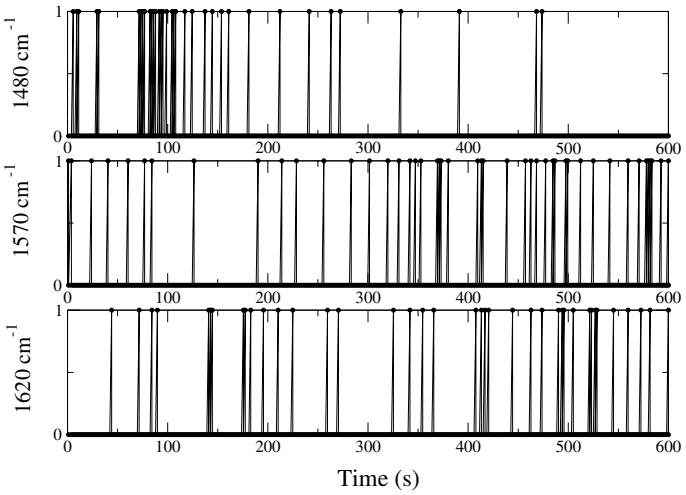


**Fig. 8.** On/off behavior of signals at the $1480\,\mathrm{cm}^{-1}$, $1570\,\mathrm{cm}^{-1}$, and $1620\,\mathrm{cm}^{-1}$ frequencies as a function of time in SM SERS of FePP. The *vertical lines* mark the spectrum number at which a signal overcoming a threshold of $2\sigma$ above the noise level of the spectrum is detected. The values of the crosscorrelation $\rho$ (see (2)) calculated between the appearance of a peak at the two different frequencies are: $\rho_{1480,1570} = 0.03$, $\rho_{1480,1620} = 0.05$, $\rho_{1570,1620} = -0.05$

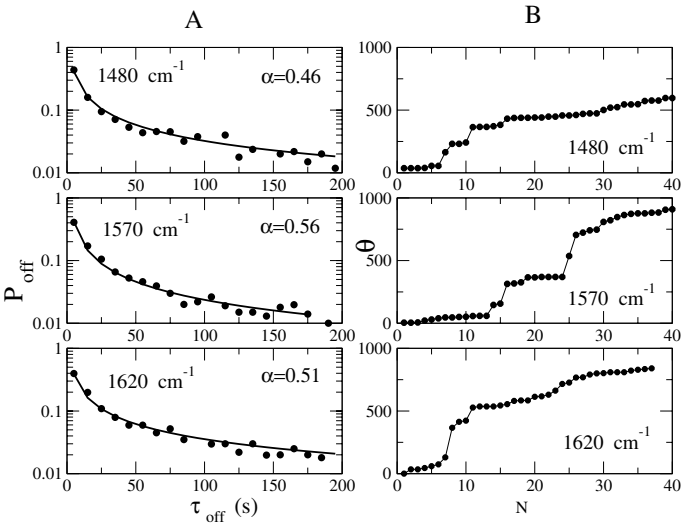


**Fig. 9.** (**a**) Distribution of the time interval $\tau_{\mathrm{off}}$ between the appearance of two successive peaks, from a collection of 10 spectra series (each series containing 600 spectra) at $1480\,\mathrm{cm}^{-1}$, $1570\,\mathrm{cm}^{-1}$, and $1620\,\mathrm{cm}^{-1}$. *Continuous curves* give the fit by $1/\tau_{\mathrm{off}}^{1+\alpha}$. (**b**) Time interval spent in the off state during the first $N$ intervals, $\theta(N)$, as a function of $N$ at the three frequencies (see (5))

expected to regulate the sampling of the FePP vibrational modes, and then of the on–off process.

Furthermore, the nonexponential trend for the $P_{\text{off}}$ distributions points to a progressive increase in the probability to detect longer off events [23]. To better investigate such an aspect, we have analyzed the overall temporal behavior of the off states by evaluating the quantity:

$$\theta(N) = \sum_{i=1}^{N} \tau_{\text{off}}(i), \tag{5}$$

which indicates the time spent in the off state during the first $N$ time intervals. Figure 9b shows the trend of $\theta$ as a function of $N$ for the three analyzed frequencies. In all cases, as time increases, longer events are observed and $\theta$ scales more rapidly than $N$.

From the statistical point of view, a power-law distribution for $P_{\text{off}}$ with an exponent between 1 and 2 (corresponding to $\alpha$ between 0 and 1), together with the peculiar trend of $\theta(N)$, can be interpreted in the framework of the Lévy statistics [54, 55]. Lévy statistics is a natural generalization of the Gaussian distribution when analyzing sums of independent, identically distributed, random variables and is characterized by a diverging variance and broad distributions with power-law tails [56, 57]. Lévy statistics, encountered in a variety of fields (economy, physics, biology, SM fluorescence emission, etc.) has been taken into account to analyze many different phenomena (laser cooling of atoms, relaxation processes of glasses, inhomogeneous line broadening, anomalous diffusion, etc.) of long-range interaction systems [21, 23, 54, 55, 58].

From the microscopic point of view, the occurrence of Lévy statistics in SM signals has been generally linked to relaxation phenomena arising from some disorder around the molecule [21]. The disorder could arise from a static, heterogeneous distribution of traps (off states) from which the molecules should escape. Alternatively, it could be due to dynamical changes in the molecule's environment, likely connected with the presence of a random walk, with a multiple pathway of the molecule onto the surface [53, 59].

The strong fluctuations in SERS signals of FePP are expected to reflect, either the intrinsic molecule dynamics determining the gating/activation of the different vibrational modes, or its interaction with the external environment. It is well known that SERS arises from a strong interaction between a molecule and its metallic substrate. Both the em and the CT enhancement mechanisms drastically depend on the details of the molecule arrangements with respect to the metal surface (position, orientation, distance, etc). Furthermore, diffusive processes of FePP on the colloidal surface could take place during the measurements [44, 60]. Accordingly, FePP molecules may experience continuously changing interactions able to modulate the emission and the gating of the vibrational modes. Indeed, SM SERS detection is reached when molecules are located near a fractal-like metal surface [61], whose com-

plex topology might give rise to anomalous diffusive processes, [62, 63], or, more specifically, to Lévy flights [22]. In this respect, we recall that the fluorescence intermittency of quantum dots, following power-law statistics, has been traced back to diffusion-controlled ET processes [64].

Therefore, the vibrational-mode emissions, which follow Lévy statistics, might originate from some heterogeneity in the molecule–colloids interactions and/or some anomalous diffusive processes, likely involving a CT.

## 4 Conclusions and Perspectives

The statistical analysis of the fluctuations appearing in SM SERS spectra has allowed us to enlighten specific phenomena usually averaged in the ensemble measurements and to disclose temporal events hidden when many different molecules are followed at the same time. In particular, our results have contributed to elucidating the role of the continuum background on the intensity fluctuations, suggesting a tight connection between these aspecific Raman signals and the SERS enhancement mechanism. The clear evidence of a switching between the two oxidation states of iron in the SM SERS spectra of FePP has led us to suggest the occurrence of a reversible ET between the molecule and the metal surface. More information about the conductive properties of a SM at the metal surface, and also their temporal variability, has been obtained by coupling SM SERS and STM measurements by adsorbing the molecule on a STM silver tip. Furthermore, it has been found that the temporal behavior of the vibrational mode emission in SM SERS spectra follows a peculiar power law. Such a trend has been traced back to a Lévy statistics whose characteristic parameters ($\alpha$-exponent, etc.) may remarkably encode significant information about the underlying photophysical processes.

In the perspective to deeper investigate the phenomena occurring at the molecule/metal interface, and to fully understand the mechanisms at the basis of SERS, it appears quite promising to conjugate SERS with other experimental techniques, such as fluorescence and STM. Actually, single molecules located in close proximity to metallic nanoparticle surfaces, exhibit fluorescence quenching or enhancement, and may undergo ET processes, likely coupled to the excitation of its vibrational modes [26, 65]. Such an approach could, therefore, offer a comprehensive view of the photophysical and -conductive properties of molecules at the metal surfaces; this information may prove rewarding also in the optonanoelectronics applications.

## References

[1] A. M. Kelley, X. Michalet, S. Weiss: Science **292**, 1671 (2001)
[2] T. Basche, W. E. Moerner, M. Orrit, U. P. Wild (Eds.): *Single-Molecule Optical Detection, Imaging and Spectroscopy* (VCH, Weinheim 1997)

[3] J. A. Veerman, M. F. Garcia-Parajo, L. Kuipers, N. F. van Hulst: Phys. Rev. Lett. **83**, 2155 (1999)
[4] C. Blum, F. Stracke, S. Becker, K. Muellen, A. J. Meixner: J. Phys. Chem. A **105**, 6983 (2001)
[5] X. S. Xie, R. C. Dunn: Science **265**, 361 B (1994)
[6] M. Moskovits: Rev. Mod. Phys. **57**, 783 (1985)
[7] A. Campion, P. Kambhampati: Chem. Soc. Rev. **27**, 241 (1998)
[8] K. Kneipp, Y. Wang, H. Kneipp, L. T. Perelman, I. Itzkan, R. R. Dasari, M. S. Feld: Phys. Rev. Lett. **78**, 1667 (1997)
[9] S. Nie, S. R. Emory: Science **275**, 1102 (1997)
[10] A. M. Michaels, M. Nirmal, L. E. Brus: J. Am. Chem. Soc. **121**, 9932 (1999)
[11] P. Hildebrandt, M. Stockburger: J. Phys. Chem. **88**, 5935 (1984)
[12] A. Otto, I. Mrozek, H. Grabhorn, W. Akemann: J. Phys.: Condens. Matter **4**, 1143 (1992)
[13] L. P. Capadona, J. Zheng, J. I. Gonzalez, T. H. Lee, S. A. Patel, R. M. Dickson: Phys. Rev. Lett. **94**, 058301 (2005)
[14] K. Kneipp, H. Kneipp, I. Itzkan, R. R. Dasari, M. S. Feld: J. Phys.: Condens. Matter **14**, R597 (2002)
[15] Y. C. Cao, R. Jin, J. M. Nam, C. S. Thaxton, C. A. Mirkin: J. Am. Chem. Soc. **125**, 14676 (2003)
[16] M. Culha, D. Stokes, L. R. Allain, T. Vo-Dinh: Anal. Chem. **75**, 6196 (2003)
[17] A. Weiss, G. Haran: J. Phys. Chem. B **105**, 12348 (2001)
[18] A. R. Bizzarri, S. Cannistraro: Chem. Phys. **290**, 297 (2003)
[19] A. R. Bizzarri, S. Cannistraro: Phys. Rev. Lett. **94**, 068303 (2005)
[20] H. Frauenfelder, F. Parak, R. D. Young: Ann. Rev. Biophys. Biophys. Chem. **17**, 451 (1988)
[21] E. Barkai, Y. J. Jung, R. Silbey: Ann. Rev. Phys. Chem. **55**, 457 (2004)
[22] P. Allegrini, P. Grigolini, B. J. West: Phys. Rev. E **54**, 4760 (1996)
[23] X. Brokmann, J. P. Hermier, G. Messin, P. Desbiolles, J. P. Bouchard, M. Dahan: Phys. Rev. Lett. **90**, 120601/1 (2003)
[24] D. M. Adams, L. Brus, C. E. D. Chidsey, S. Creager, C. Creutz, C. R. Kagan, P. V. Kamat, M. Lieberman, S. Lindsay, R. A. Marcus, R. M. Metzger, M. E. Michel-Beyerle, J. R. Miller, M. D. Newton, D. R. Rolison, O. Sankey, K. S. Schanze, J. Yardley, X. Zhu: J. Phys. Chem. B **107**, 6668 (2003)
[25] A. R. Bizzarri, S. Cannistraro: J. Phys. Chem. B **109**, 16571 (2005)
[26] M. W. Holman, R. Liu, D. M. Adams: J. Am. Chem. Soc. **125**, 12649 (2003)
[27] C. Joachim, J. K. Gimzewski, A. Aviram: Nature **408**, 541 (2000)
[28] P. C. Lee, D. J. Meisel: J. Phys. Chem. **86**, 3391 (1982)
[29] A. R. Bizzarri, S. Cannistraro: Appl. Spectrosc. **56**, 1531 (2002)
[30] A. R. Bizzarri, S. Cannistraro: Chem. Phys. Lett. **349**, 503 (2001)
[31] I. Delfino, A. R. Bizzarri, S. Cannistraro: Biophys. Chem. **113**, 41 (2003)
[32] H. Xu, E. J. Bjerneld, M. Kaell, L. Boerjesson: Phys. Rev. Lett. **83**, 4357 (1999)
[33] E. J. Bjerneld, Z. Foeldes-Papp, M. Kaell, R. Rigler: J. Phys. Chem. B **106**, 1213 (2002)
[34] S. Habuchi, M. Cotlet, R. Gronheid, G. Dirix, J. Michiels, J. Vanderleyden, F. C. De Schryver, J. Hofkens: J. Am. Chem. Soc. **125**, 8446 (2003)
[35] K. A. Bosnick, J. Jiang, L. E. Brus: J. Phys. Chem. B **106**, 8096 (2002)

[36] A. Otto: J. Raman Spectrosc. **33**, 593 (2002)
[37] E. J. Bjerneld, F. Svedberg, P. Johansson, M. Kaell: J. Phys. Chem. A **108**, 4187 (2004)
[38] P. Hildebrandt, M. Stockburger: Vib. Spectra. Struct. **17**, 443 (1986)
[39] J. R. Taylor: *An Introduction to Error Analysis* (University Science Books, Sausalito 1982)
[40] A. A. Moore, M. L. Jacobson, N. Belabas, K. L. Rowlen, D. M. Jonas: J. Am. Chem. Soc. **127**, 7292 (2005)
[41] J. R. Lakowicz, J. Malicka, S. D. Auria, I. Gryczynski: Anal. Biochem. **320**, 13 (2003)
[42] B. N. Persson: Chem. Phys. Lett. **82**, 561 (1981)
[43] F. Moresco, G. Meyer, K. H. Rieder, H. Tang, A. Gourdon, C. Joachim: Phys. Rev. Lett. **86**, 672 (2001)
[44] Y. He, T. He, E. Borguet: J. Am. Chem. Soc. **124**, 11964 (2002)
[45] H. M. Marques, K. L. Brown: Coord. Chem. Rev. **225**, 123 (2002)
[46] S. Rywkin, C. M. Hosten, J. R. Lombardi, R. L. Birke: Langmuir **18**, 5869 (2002)
[47] A. R. Bizzarri, S. Cannistraro: Chem. Phys. Lett. **395**, 222 (2004)
[48] I. Lee, J. W. Lee, E. Greenbaum: Phys. Rev. Lett. **79**, 3294 (1997)
[49] N. J. Tao: Phys. Rev. Lett. **76**, 4066 (1996)
[50] W. Han, E. N. Durantini, T. A. Moore, A. L. Moore, D. Gust, P. Rez, G. Leatherman, G. R. Seely, N. J. Tao, S. M. Lindsay: J. Phys. Chem. B **101**, 10719 (1997)
[51] A. M. Michaels, J. Jiang, L. Brus: J. Phys. Chem. B **104**, 11965 (2000)
[52] M. Kuno, D. P. Fromm, H. F. Hamann, A. Gallagher, D. J. Nesbitt: J. Chem. Phys. **112**, 3117 (2000)
[53] M. Nirmal, B. O. Dabbousi, M. G. Bawendi, J. J. Macklin, J. K. Trautman, T. D. Harris, L. E. Brus: Nature **383**, 802 (1996)
[54] W. Feller: *An Introduction to Probability Theory and Its Applications* (Wiley, New York 1970)
[55] M. Shlesinger, G. M. Zaslavsky, U. Frisch (Eds.): *Lévy Flights and Related Topics in Physics* (Springer, Berlin, Heidelberg 1995)
[56] A. M. Stoneham: Rev. Mod. Phys. **41**, 82 (1969)
[57] G. Wornell: *Signal Processing with Fractals* (Prentice Hall PTR, Upper Saddle River 1995)
[58] F. Bardou, J. P. Bouchaud, A. Aspect, C. Cohen-Tannoudji: *Lévy Statistics and Laser Cooling* (Cambridge Univ. Press, Cambridge 2002)
[59] K. T. Shimizu, R. G. Neuhauser, C. A. Leatherdale, S. A. Empedocles, W. K. Woo, M. G. Bawendi: Phys. Rev. B **63**, 205316 (2001)
[60] T. Komeda, Y. Kim, M. Kawai, B. N. J. Persson, H. Ueba: Science **295**, 2055 (2002)
[61] Z. Wang, S. Pan, T. D. Krauss, H. Du, L. J. Rothberg: Proc. Natl. Acad. USA **100**, 8638 (2003)
[62] J. M. Sancho, A. M. Lacasta, K. Lindenberg, I. M. Sokolov, A. H. Romero: Phys. Rev. Lett. **92**, 250601 (2004)
[63] M. Schunack, T. R. Linderoth, F. Rosei, E. Laegsgaard, I. Stensgaard, F. Besenbacher: Phys. Rev. Lett. **88**, 156102 (2002)
[64] J. Tang, R. A. Marcus: Phys. Rev. Lett. **95**, 107401 (2005)

[65] B. C. Stipe, M. A. Rezaei, W. Ho: Science **280**, 1732 (1998)
[66] P. Etchegoin, H. Liem, R. C. Maher, L. F. Cohen, R. J. C. Brown, H. Hartigan, M. J. T. Milton, J. C. Gallop: Chem. Phys. Lett. **366**, 115 (2002)

## Index